

Electronic and magnetic properties of SrRu₂O₆*

Satoshi Okamoto,^{1,†} Masayuki Ochi,^{2,3} Ryotaro Arita,³ Jiaqiang Yan,¹ and Nandini Trivedi⁴

¹*Materials Science and Technology Division, Oak Ridge National Laboratory, Oak Ridge, Tennessee 37831, USA*

²*Department of Physics, Graduate School of Science, Osaka University, Osaka 565-0843, Japan*

³*RIKEN Center for Emergent Matter Science (CEMS), Hirosawa, Wako, Saitama 351-0198, Japan*

⁴*Department of Physics, The Ohio State University, Columbus, Ohio 43210, USA*

Electron correlations tend to generate local magnetic moments that usually order if the lattices are not too frustrated. The hexagonal compound SrRu₂O₆ has a relatively high Néel temperature but small local moments, which seems to be at odds with the nominal valence of Ru⁵⁺ in the t_{2g}^3 configuration. Here, we investigate the electronic and magnetic properties of SrRu₂O₆ using density functional theory (DFT) combined with dynamical mean field theory (DMFT). We find that the strong hybridization between Ru d and O p states results in a Ru valence that is closer to +4, leading to the small ordered moment, consistent with a DFT prediction. While the agreement with DFT might indicate that SrRu₂O₆ is in the weak coupling regime, our DMFT studies provide evidence from the mass enhancement and local moment formation that indicate correlation effects play a significant role. The local moment per Ru site is nearly identical to the ordered moment at low temperatures and remains finite in the whole temperature range investigated. Our theoretical Néel temperature ~ 700 K is in reasonable agreement with experimental observations. Due to a small lattice distortion, the degenerate t_{2g} manifold is split and the quasiparticle weight is renormalized significantly in the a_{1g} state, while correlation effects in e'_g states are about a factor of 2-3 weaker. SrRu₂O₆ is a unique system in which the itinerant band picture and Mott physics coexist with an orbitally-selective Mott transition within the t_{2g} sector.

Introduction

For systems with an odd number of electrons per unit cell, correlation effects can lead to insulating magnetic ground states. Depending on the relative strength between the interactions U and the electron bandwidth or kinetic energy W , there are two classes of insulators: A Slater insulator[1] in the weak coupling regime in which the normal state is a non-magnetic metal. Below a critical temperature a gap in the single-particle opens up because of magnetic ordering and consequently the unit cell gets doubled and the Brillouin zone folds up. In this regime, the magnetic transition temperature increases with increasing Coulomb interaction strength. In the opposite strong coupling regime, the system is a Mott insulator[2, 3]. In this limit, the normal state is a gapped insulator due to strong Coulomb repulsion. Magnetic ordering sets in below a critical temperature $T_c \sim W^2/U$ related to the superexchange scale[4]. Interpolating between these two limits, the maximum T_c is expected to occur in the crossover regime where U and W are com-

parable.

The behavior of T_c in a series of perovskite transition-metal oxides (TMOs) with the formal t_{2g}^3 electron configuration, including SrMnO₃, SrTcO₃ and NaOsO₃, lend support to the above picture. $3d$ TMO SrMnO₃ has a relatively low Néel temperature $T_N = 260$ K [5] for antiferromagnetic (AF) ordering but the insulating behavior persists above T_N , indicating that it is in the strong coupling limit. On the other hand, $5d$ TMO NaOsO₃ with an AF transition $T_N = 410$ K and a metal-insulator transition that is coincident [6] appears to be in the weak coupling limit. Finally, $4d$ TMO SrTcO₃ shows extremely high AF $T_N \sim 1000$ K [7], which indicates it is located in the crossover regime [8].

Given this backdrop, an important question that arises is *can there be systems that are incompatible with this classification?* And more broadly, what are the criteria for weak coupling Slater and strong coupling Mott regimes in multi-orbital systems?

One such systems is pyrochlore Cd₂Os₂O₇. As in NaOsO₃, the metal-insulator transition of Cd₂Os₂O₇ accompanies a magnetic ordering [9, 10]. However, unlike NaOsO₃ the unit cell of Cd₂Os₂O₇ contains four Os sites and, therefore can become an insulator without changing the size of the unit cell. In fact, the observed all-in-all-out magnetic structure is compatible with the structural unit cell [11, 12]. It turns out that the metal-insulator transition in Cd₂Os₂O₇ is a Lifshitz transition [13] arising from a reconstruction of the Fermi surface, rather than a Slater transition.

In this paper, we focus on another compound, the hexagonal SrRu₂O₆ [14] [Fig. 1 (a)]. We may expect that given a half filled t_{2g} configuration for Ru sites from its formal valence +5, like Os⁵⁺ in NaOsO₃ or Cd₂Os₂O₇

*Copyright notice: This manuscript has been authored by UT-Battelle, LLC under Contract No. DE-AC05-00OR22725 with the U.S. Department of Energy. The United States Government retains and the publisher, by accepting the article for publication, acknowledges that the United States Government retains a non-exclusive, paid-up, irrevocable, world-wide license to publish or reproduce the published form of this manuscript, or allow others to do so, for United States Government purposes. The Department of Energy will provide public access to these results of federally sponsored research in accordance with the DOE Public Access Plan (<http://energy.gov/downloads/doe-public-access-plan>)

[†]okapon@ornl.gov

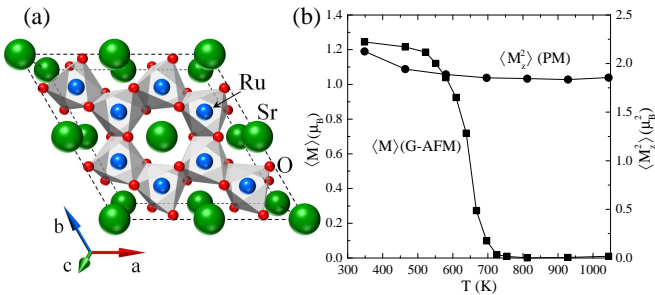


FIG. 1: (a) Top view of SrRu_2O_6 . The cell is doubled along the a and b directions. (b) Ordered $\langle M \rangle$ and equal-time spin-spin correlation $\langle M_z^2 \rangle$ as a function of temperature T . From the high temperature value, $\langle M_z^2 \rangle \sim 1.8\mu_B^2$, the local moment is estimated to be $M \sim 2.3\mu_B$.

and also because Ru is a $4d$ element, it may show behavior similar to SrTcO_3 . Indeed, a fairly high $T_N \sim 565$ K is observed in SrRu_2O_6 [15]. However, the ordered moment $\sim 1.3\mu_B$ is found to be much smaller than that expected for Ru^{5+} , $3\mu_B$ [15, 16]. To solve this puzzle, there have appeared a number of theoretical studies using density functional theory (DFT). Singh [17] and Tian *et al.* [15] argued that the strong hybridization between Ru and O ions is responsible for the reduction of ordered moment. Streltsov and coworkers proposed the formation of molecular orbitals within a Ru hexagonal plane owing to such a strong hybridization [18]. They also performed the DFT calculation combined with the dynamical mean field theory [19] (DFT+DMFT [20–22]). It was reported that the ordered moment on a Ru site becomes $3\mu_B$ as anticipated for Ru^{5+} and that the transition temperature becomes ~ 2000 K, which is very similar to a theoretical result for SrTcO_3 [8] and in return supports the importance of the molecular orbital picture that are not considered in DMFT.

In this paper, we investigate the electronic and magnetic property of SrRu_2O_6 using DFT+DMFT. Our main finding is summarized in Fig. 1 (b). In contrast to the previous report of Ref. [18], we find that the ordered moment is indeed $\sim 1.2\mu_B$, which is nearly identical to the DFT result $1.3\mu_B$ [17] and also consistent with the experimental value $1.4\mu_B$ [15, 16]. These observation might indicate that SrRu_2O_6 is in the weak coupling limit, similar to NaOsO_3 , not in the crossover regime. However, the local moment estimated by the equal-time spin-spin correlation remains relatively large throughout the temperature range analyzed. We also find that the transition temperature estimated from DMFT is $T_N \sim 700$ K, reasonably close to the experimental $T_N \sim 565$ K [15, 16]. Fluctuations not included in DMFT are expected to reduce the ordering temperature bringing it closer to the experimental estimate. Even more significantly, we find that one of t_{2g} states shows strong mass enhancement. Thus, our results indicate SrRu_2O_6 is in close proximity to an orbitally-selective Mott insulating state.

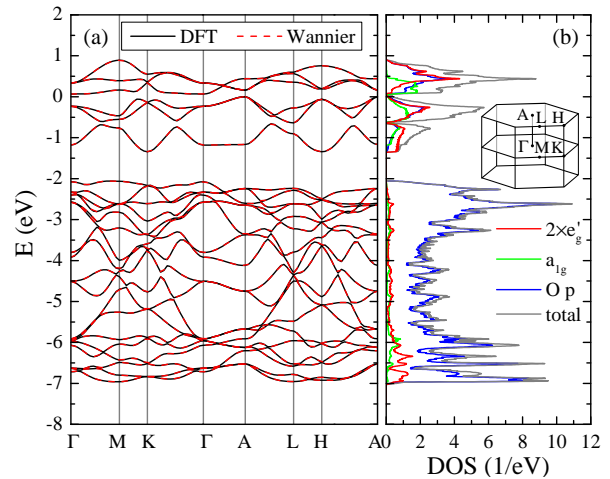


FIG. 2: DFT results on SrRu_2O_6 . (a) Band dispersion (solid lines) compared with Wannier dispersions (broken lines). (b) Total and orbital-resolved (Ru e'_g , a_{1g} and O p) DOS. The valence-band maximum is set to $E = 0$. DOS for e'_g involves contributions from two degenerate bands. The inset shows the first Brillouin zone for the hexagonal lattice.

Results

DFT analysis

We utilize DFT+DMFT techniques [20–22] to better account for correlation effects associated with the localized Ru d electrons. We first perform the DFT calculations for the non-magnetic state with the Elk package [23]. The experimental lattice parameters are considered with atomic configurations determined at room temperature [14]. It turns out that these calculations themselves provide important insights into the novel behavior of SrRu_2O_6 .

Within the DFT, a small band gap ~ 0.05 eV exists at the Fermi level in a paramagnetic state [15], indicating that SrRu_2O_6 is a band insulator.

We then construct a model Hamiltonian consisting of Ru t_{2g} states and O p states using the Wannier functions [24–27] and transfer integrals between them on different sites extracted from the DFT band structure. We estimate the interaction parameters from the constrained random phase approximation (cRPA) [28]. Details of our model construction are provided in the Methods section. The interacting model thus obtained is solved by means of DMFT with the continuous-time quantum Monte-Carlo impurity solver [29–31].

It is instructive to start from the DFT results as summarized in Fig. 2. Fig. 2 (a) shows the DFT dispersion relations near the Fermi level. The valence-band maximum is set to $E = 0$. The first Brillouin zone for the hexagonal lattice is shown as an inset of Fig. 2 (b). In this calculation, magnetic ordering is suppressed. RuO_6 octahedra are slightly compressed along the c direction,

and O-Ru-O angle is about 94.4° (two oxygen sites are on the same plane). Reflecting this distortion and the hexagonal symmetry, i.e., a_{1g} and e'_g are intrinsically inequivalent, the a_{1g} level is about 0.3 eV higher than the e'_g level.

These bands are well separated from the other bands located below -15 eV or above $+3$ eV. As shown in Fig. 2 (b), these bands primarily come from Ru t_{2g} states (split to twofold degenerate e'_g states and non-degenerate a_{1g} states) and O p states, justifying our choice of the basis set of the model Hamiltonian. It is clearly seen that Ru t_{2g} and O p states are strongly hybridized in the energy window $[-7.0; +1.0]$ eV. Interestingly, the substantial amount of O p states are above the Fermi level, corresponding to 2.596 holes in the O p states per unit cell or 0.433 holes per oxygen ion. This point will become crucial in the discussion below. It should also be mentioned that Ru a_{1g} states have the largest weight near the Fermi level (Note that Ru e'_g states have the twofold degeneracy, therefore each e'_g band has the smaller spectral weight than the a_{1g} band near the Fermi level). This indicates that the effect of correlations is different between e'_g and a_{1g} states.

The left panel also shows the Wannier dispersion relations, which completely overlap with the DFT dispersion relations. There are 48 bands including the spin degeneracy, i.e., 6 per Ru (t_{2g}) and 6 per O (p_x, p_y, p_z). A Sr does not contribute to these low-energy bands because Sr $5s(4p)$ level is so high (low) and its valence state is $+2$ by donating 2 electrons to these bands. Considering the nominal valence, $\text{Sr}^{2+}\text{Ru}_2^5+\text{O}_6^{2-}$, and the charge counting, 3 per Ru^{5+} and 6 per O^{2-} , these bands are filled by 42 electrons. Within DFT, the filling is about 1.42 per a_{1g} orbital and about 1.45 per e'_g orbital, so these orbitals are nearly equally filled.

Double counting correction

For methods using DFT supplemented by many-body calculations, it is critical that we first correct for the Hartree contribution arising from correlated orbitals that is already included in the DFT calculation; we call this the double-counting correction (DC). This is introduced as a uniform level shift of correlated orbitals ε_{DC} . Two methods for accounting for such a DC correction have been investigated during the development of local (spin) density approximation [L(S)DA] $+U$ methods [32, 33]. Since the combination of DFT+ DMFT techniques started to appear, a number of DC correction methods have been proposed [34–39]. However, it remains unclear which of these methods is best suited for the current system. Here, instead of examining each DC method, we take a different approach: we treat ε_{DC} as an adjustable parameter and based on the experimental input, i.e., the ordered moment, determine the parameter range suitable for the material and then used for the more detailed calculations of the quasi-particle weight.

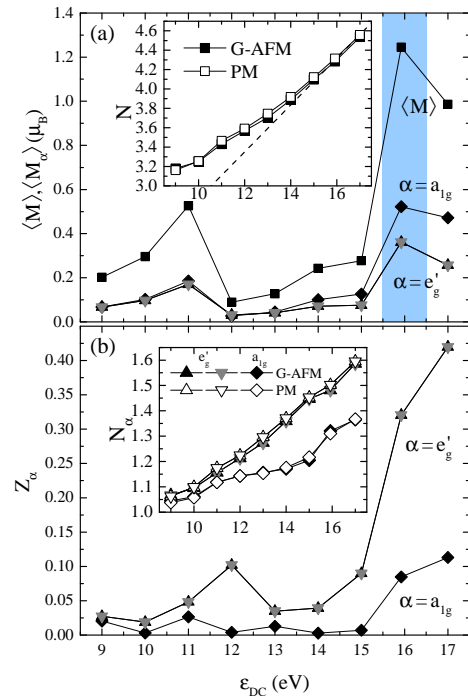


FIG. 3: (a) DMFT results of the total and the orbital-resolved ordered magnetic moments, $\langle M \rangle$ and $\langle M_\alpha \rangle$, respectively, as a function of ε_{DC} . (b) Quasiparticle weight Z_α as a function of ε_{DC} . The insets of (a) and (b) respectively show the total d electron density N and the orbital-resolved density N_α as a function of ε_{DC} .

The inset of Figure 3 (a) [(b)] shows the total (orbital-resolved) Ru d electron density N (N_α) as a function of ε_{DC} . As one can see, the total density N remains larger than 3, the nominal value for Ru^{5+} , for the whole ε_{DC} range examined and, to realize $N = 3$, i.e., the d^3 electron configuration, ε_{DC} must be unrealistically small. N and N_α are not sensitive to the magnetic state, compare paramagnetic (PM) solutions and G-type antiferromagnetic (G-AFM) solutions. In all ε_{DC} , a_{1g} orbitals have electron density closer to 1 than e'_g orbitals. From this, one could anticipate that a_{1g} electrons contribute to magnetism more strongly than e'_g electrons.

In the inset of Fig. 3 (a), we also plot the analytical line

$$\varepsilon_{DC} = U_{ave} \left(N - \frac{1}{2} \right) - \frac{1}{2} J_{ave} (N - 1), \quad (1)$$

which is the so-called fully localized limit (FLL) [32], with U_{ave} and J_{ave} being averaged Coulomb interaction and exchange interaction computed from matrix elements presented in the Method section, Eqs. (4) and (5), respectively. We notice that the analytic curve and the numerical data practically overlap at $\varepsilon_{DC} \gtrsim 15$ eV. Thus, if one takes the FLL DC correction and imposes the condition that impurity occupation N and the one in the DC correction Eq. (1) coincide, any point at $\varepsilon_{DC} \gtrsim 15$ eV

fulfills this condition. This means that the full convergence for this scheme is very difficult. Instead of proceeding this, we take the Ru d occupancy from the DFT calculation, $N = 4.3$, and use this value in Eq. (1) to obtain $\varepsilon_{DC} = 15.92$ eV. This ε_{DC} gives impurity occupancy $N = 4.28(4.31)$ in the PM (G-AFM) solution at $T = 348$ K. It is reported that the FLL formula gives a slightly larger impurity occupancy than the “nominal” DC (in this case $N = 3$), which is close to the “exact” DC [39]. However, the true nominal occupancy in Ru d states is not known, yet. While it remains to be justified to use the FLL DC with $N = 4.3$, our results suggest that our choice of ε_{DC} provide reasonable physical picture of SrRu₂O₆. It is very interesting to apply the improved DC correction to SrRu₂O₆, but this remains to be a future research.

Given the vital information on the Ru d occupation number N vs. ε_{DC} in the inset of Fig. 3 (a), we examine physical quantities as a function of ε_{DC} . Figure 3 (a) shows the total magnetization $\langle M \rangle$ and orbital-resolved ordered moment $\langle M_\alpha \rangle$ for G-AFM as a function ε_{DC} . Here, $\langle M \rangle = \sum_\alpha \langle M_\alpha \rangle$ with $\langle M_\alpha \rangle = N_{\alpha\uparrow} - N_{\alpha\downarrow}$. One notices that the ordered moment on the a_{1g} orbital is larger compared to the e'_g orbitals. This is because the a_{1g} occupation is closer to one than the e'_g occupations [see the inset of Figure 3 (b)].

The ordered moment varies drastically with ε_{DC} mainly because a_{1g} level is about 0.3 eV higher than the e'_g level and the a_{1g} orbital is less populated than e'_g orbitals [see Fig. 3 (b) inset]. As a result, the system has a tendency towards the orbital polarization, $N_{a_{1g}} < N_{e'_g}$. It is known that the the orbital polarization is enhanced by correlations [40, 41], leading to the smaller $N_{a_{1g}}$. Furthermore, as shown later, spectral weight right below the Fermi level is dominated by a_{1g} orbital [Fig. 4 (a)]. Since reducing ε_{DC} roughly corresponds to lowering E_F , a_{1g} orbital changes the occupation number more sensitively than e'_g orbitals.

The experimental value of the ordered moment $1.4\mu_B$ [15, 16] suggests that $N \sim 4.3$ is the realistic value, corresponding to $\varepsilon_{DC} = 15.92$ eV. This is quite different from the nominal occupation of Ru⁵⁺, $N = 3$. Such a large difference of N from its nominal value comes from the strong mixture between Ru d states and O p states in low-energy bands. It should be noted that in order to achieve $N = 3$, one needs to adopt unphysically small ε_{DC} .

The magnetic behavior appears to suggest that SrRu₂O₆ is in the weak coupling regime despite relatively large values of the matrix elements of \hat{U} . This is because e'_g orbitals are more extended within the ab plane and more strongly hybridized with the surrounding oxygen p states than a_{1g} orbital, and therefore have wider band width. Moreover, e'_g states have spectral functions with suppressed weight at the Fermi level. This feature indicates that the charge fluctuation as well as the correlation effects are suppressed. But, is this true? Thus, we now turn to the quasiparticle weight, which is the direct

measure of the correlation strength. Figure 3 (b) shows orbital dependent quasiparticle weight Z_α as a function of ε_{DC} . It is seen that Z_α for $\alpha = a_{1g}$ becomes extremely small at $\varepsilon_{DC} < 10$ eV and $\varepsilon_{DC} \sim 14$ eV corresponding to integer fillings $N = 3$ and 4, respectively, while Z_α for $\alpha = e'_g$ remains larger than 0.02. This indicates that the correlation effect is quite strong and the system is in the vicinity of orbital-selective Mott insulating regimes [42], in which $\alpha = a_{1g}$ electrons are localized but e'_g electrons maintain the itinerant character. This also reminds us of the bad-metal behavior in an extended range of coupling and carrier densities in strongly-correlated multiorbital systems in the presence of Hund’s coupling [43, 44].

In many magnetic materials, the ordered moment increases with increasing the correlation strength. Thus, the quasiparticle weight in a PM solution and the ordered moment in a magnetic solution tend to have a negative correlation. As shown in Figs. 3 (a) and (b), on the contrary, the ordered moments become large where the quasiparticle weights become large, i.e., they have a positive correlation. All these observations suggest that SrRu₂O₆ is in the strong coupling regime, but Mott physics and itinerant band physics coexist.

We also note here that while DFT+DMFT calculations on SrRu₂O₆ have also been reported in Ref. [18], our results are quite different: Ref. [18] finds a large Ru moment $\sim 3\mu_B$ and the extremely high transition temperature ~ 2000 K. While sufficient details are not provided in Ref. [18], we suspect from our calculations that the main difference arises from the inclusion of ligand O p states in our calculations that are crucial to describe the electronic properties of the late transition-metal oxides with deeper d levels.

Now, we check the low-temperature electronic property. Figure 4 (a,b) show the Ru d density of states computed by the maximum entropy analytic continuation for the impurity Green’s functions on the Matsubara axis [45]. e'_g states have a clear gap in both PM and G-AFM solutions with the peak-to-peak distance ~ 0.6 eV and ~ 0.9 eV, respectively. For a_{1g} states, a gap structure is rather vague especially in the PM solution. The minimum peak-to-peak distance is ~ 0.2 eV for both PM and G-AFM. This is comparable to the experimental estimate on the activation energy ~ 0.4 eV [15].

As a closely related system, SrTcO₃ was studied in Ref. [7]. The experimental ordered moment is found to be $2.13(1.87)\mu_B$ at low (room) temperature. The ordered moment deduced by DFT is $1.3\mu_B$. All these values are substantially smaller than $S = 3/2$ moment $3.87\mu_B$. SrTcO₃ as well as SrMnO₃, both of which are d^3 systems, were examined using DFT+DMFT in Ref. [8]. The ordered moment is found to be $2.5\mu_B$ for SrTcO₃ and $3\mu_B$ for SrMnO₃ at low temperatures. These values are close to the experimental values. The local moment for the two materials are estimated from $\langle S_{zi}^2 \rangle$ above T_N to be $2.7\mu_B$ for the Tc and $3.8\mu_B$ for Mn compound. The paramagnetic magnetic moment of Mn is close to the maximal value $3.87\mu_B$, while that for Tc is suppressed

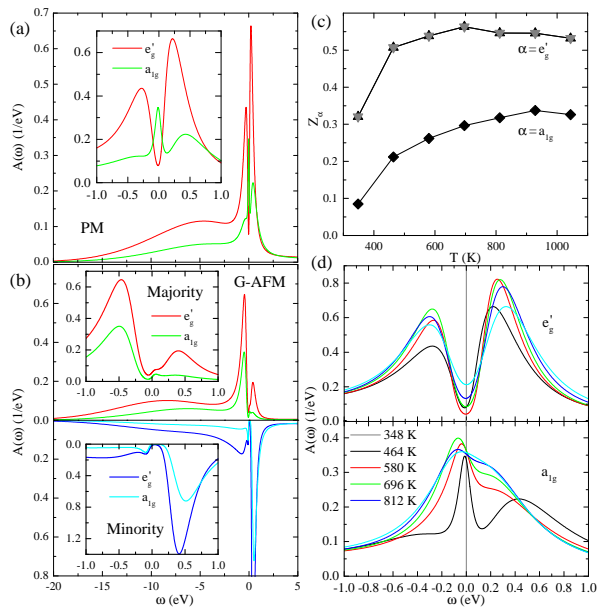


FIG. 4: : DMFT results of the spectral function $A_\alpha(\omega)$ for a PM phase (a) and a G-AFM phase (b) at $T = 348$ K. (c) Orbital-resolved quasiparticle weight Z_α as a function of T . The a_{1g} band shows the stronger mass enhancement than the e_g band by a factor of 2–3. (d) Temperature dependent spectral function $A_\alpha(\omega)$.

because of the more-itinerant nature of SrTcO_3 . The reported dependence of ordered and local moments on the “B” site elements of perovskite SrBO_3 is consistent with the Slater-Mott crossover for half-filled Hubbard models. Our results on SrRu_2O_6 are closer to SrTcO_3 than SrMnO_3 . However, the reduction from the local moment to the ordered moment is much stronger $1.3/2.3 \sim 0.57$ for our SrRu_2O_6 as compared with $2.5/2.7 \sim 0.93$ for SrTcO_3 . This clearly indicates the importance of the coexistence of Mott and itinerant electrons or orbital-selective Mott/magnetism in SrRu_2O_6 .

Temperature dependence

We now move on to the temperature dependence.

Magnetic properties are summarized in Fig. 1 (b). Local ordered moment $\langle M \rangle$ is computed for G-type AFM and plotted as a function of temperature. At a glance, one notices a close resemblance between the theoretical $\langle M \rangle$ vs. T curve and experimental ones reported in Refs. [15, 16]. Theoretical results for the ordered moment at low temperatures is $\langle M \rangle \sim 1.2\mu_B$ and the Néel temperature $T_N \sim 700$ K are rather consistent with the experimental results, $\langle M \rangle \sim 1.4\mu_B$ and $T_N \sim 565$ K. Theoretical T_N is overestimated by about 20 %, which could be reasonably attributed to the mean field nature of the current “single-site” DMFT and the uniaxial anisotropy existing in real material but absent in our calculations.

In Slater-type systems in the weak coupling limit, local moments disappear when magnetic ordering disappears above T_N . On the other hand in Mott insulators in the strong coupling limit, local moments remain unchanged above T_N . In the intermediate crossover regime, local moments decrease with increasing temperature but survive at high temperatures. We have also computed the equal-time spin-spin correlation in an impurity model $\langle M_z^2 \rangle = \langle |\sum_\alpha N_{\alpha\uparrow} - N_{\alpha\downarrow}|^2 \rangle$. As shown in Fig. 1 (b), $\langle M_z^2 \rangle$ remains constant $\approx 1.8 \mu_B^2$ in the whole temperature range. Moreover, the size of the local moment deduced from this value is $|M_z| = \langle M_z^2 \rangle \approx 1.34\mu_B$, which roughly coincides with the size of the ordered moment at low temperatures. Thus, clearly SrRu_2O_6 is not in the weak-coupling limit but most likely in the strong-coupling limit; even if it is in the intermediate crossover regime, it would be very close to the strong coupling regime. Similar dichotomy between large local moments and small ordered magnetic moments in was theoretically suggested for iron-based superconductors [46, 47] and has indeed been experimentally reported [48].

This is also confirmed by the temperature dependent quasiparticle weight. As shown in Fig. 4 (c), Z_s in PM solutions are decreased with decreasing T . This behavior contradicts with the expectation for a good metal where the electron coherence is enhanced with decreasing temperature. It is also interesting to point out that the renormalization in $Z_{e'_g}$ is moderate for high temperatures. This is because e'_g bands maintain the band-insulator-like character and have larger spectral weights away from $\omega = 0$. On the other hand, the renormalization in $Z_{a_{1g}}$ is significant. Thus, SrRu_2O_6 is in the vicinity of the correlation-induced orbital-selective Mott transition.

Discussion

Because of the large imaginary part of the self-energies, it remains challenging to identify the low-energy feature of the spectral function. Nevertheless, the temperature dependence of $A_\alpha(\omega)$ might give a hint of the transport property. As shown in Fig. 4 (d), e'_g bands show the gapped feature and, therefore, do not contribute to the transport much. On the other hand, the spectral function for the a_{1g} band is gradually diminished at $\omega \sim 0$ with decreasing temperature. Thus, we expect the electric resistivity to increase with decreasing temperature in the whole temperature range, including $T \gg T_N$.

In the weak-coupling picture, SrRu_2O_6 is a band insulator at both above and below T_N , the gap amplitude is fixed at $T > T_N$ and grows rapidly according to the magnetic order parameter at $T < T_N$. Therefore, $\rho(T)$ curve is expected to have a kink at T_N . On the other hand in our strong coupling picture, the spectral functions evolve dynamically even in the PM regime. Due to the large self-energy or scattering rate, details of low-energy feature in $A(\omega)$ are smeared out. Thus, $\rho(T)$ is expected to

change smoothly across T_N .

To verify our results, it would be very important to experimentally examine the resistivity in the whole temperature range, from $T \ll T_N$ to $T \gg T_N$. The preliminary results on the resistivity above room temperature appear to support this [49]. Also, (angle resolved) photoemission spectroscopy measurements would provide the direct evidence of the dynamical change in the spectral function, the evolution of the pseudogap feature to the full gap with decreasing temperature across T_N .

The current work suggests that SrRu_2O_6 has to be considered as a different class of material than a series of t_{2g}^3 TMOs, including SrMnO_3 , SrTcO_3 and NaOsO_3 , where the low-energy behavior is well captured by multi(3)-orbital Hubbard models. To understand the unique behavior of SrRu_2O_6 , it is essential to consider strong hybridization between Ru d and O p states. This could largely modify the T vs. U phase diagram by reducing both T_N and the local moment M_{loc} , while the correlation strength in TM d states remains strong. There might be a large number of materials that could be classified into a similar category as SrRu_2O_6 .

To summarize, we have investigated the novel electronic and magnetic properties of hexagonal compound SrRu_2O_6 using DFT+DMFT. The small moment on Ru $\sim 1.2\mu_B$ and the relatively high Néel temperature ~ 700 K are consistent with the experimental report, $\sim 1.4\mu_B$ and $T_N \sim 565$ K. These seemingly contradictory characters of SrRu_2O_6 are caused by the strong hybridization between Ru d states and ligand O p states, which increases the Ru d occupancy substantially from the nominal value 3. The strong Ru d -O p hybridization does not imply the weak-coupling nature. In fact, SrRu_2O_6 is in the strong-coupling regime, in the verge of the Mott localization. While the DFT calculations predict a band insulator when magnetic ordering is suppressed. On the contrary, we predict that the electron spectral functions evolve dynamically with temperature. In particular above Néel temperature, the spectral functions exhibit pseudogap feature, which turns to full gap with decreasing temperature. To verify our predictions, further experimental studies are desirable, including temperature dependent photoemission spectroscopy measurements and resistivity measurements.

Method

DFT calculation was performed for the non-magnetic state with the Elk package [23] using the exchange-correlation functional proposed by Perdew *et al.* [50]. We considered the experimental lattice parameters and atomic configurations determined at room temperature [14].

Using the obtained band structure, we constructed the

Wannier functions [24–27] containing the Ru t_{2g} and O p orbitals and calculated the transfer integrals among them. The energy window was set as $[-7.0; +1.0]$ eV. Further, we evaluated the interaction parameters, the Coulomb repulsion \hat{U} and the exchange coupling \hat{J} , by the constrained random phase approximation (cRPA) [28]. In the calculation of the partially screened Coulomb interaction, we took 120 unoccupied bands and used a $4 \times 4 \times 4$ grid. The double Fourier transform of the constrained susceptibility was done with the cutoff of 5 (1/a.u.). For simplicity, we neglected the spin-orbit interaction, since it is irrelevant in our analyses. These calculations were performed using a density response code [51] recently developed for the Elk branch of the original EXCITING FP-LAPW code [23].

The obtained effective model consists of two parts $H = H_{band} + \sum_{i \in \text{Ru}} H_{int,i}$. The band part H_{band} is given by

$$H_{band} = \sum_{\vec{k}, \sigma} \left[\hat{d}_{\vec{k}\sigma}^\dagger, \hat{p}_{\vec{k}\sigma}^\dagger \right] \begin{bmatrix} \hat{\epsilon}_{\vec{k}}^{dd} - \varepsilon_{DC} \hat{1} & \hat{\epsilon}_{\vec{k}}^{dp} \\ \hat{\epsilon}_{\vec{k}}^{pd} & \hat{\epsilon}_{\vec{k}}^{pp} \end{bmatrix} \begin{bmatrix} \hat{d}_{\vec{k}\sigma} \\ \hat{p}_{\vec{k}\sigma} \end{bmatrix}. \quad (2)$$

Here, $\hat{d}_{\vec{k}\sigma}$ ($\hat{p}_{\vec{k}\sigma}$) is a vector consisting of annihilation operators of Ru t_{2g} (O p) electrons with spin σ in a momentum \vec{k} space. The dispersion $\hat{\epsilon}_{\vec{k}}^{\alpha\beta}$ consists of Wannier parameters, with α and β running through Ru t_{2g} and O p states. ε_{DC} for interacting Ru t_{2g} states is the DC correction.

The interaction part H_{int} is given by

$$H_{int} = \sum_a U_{aa} d_{a\uparrow}^\dagger d_{a\uparrow} d_{a\downarrow}^\dagger d_{a\downarrow} + \sum_{a \neq b} U_{ab} d_{a\uparrow}^\dagger d_{a\uparrow} d_{b\downarrow}^\dagger d_{b\downarrow} \\ + \sum_{a > b, \sigma} (U_{ab} - J_{ab}) n_{a\sigma} n_{b\sigma} \\ + \sum_{a \neq b} J_{ab} \left(d_{a\uparrow}^\dagger d_{b\uparrow} d_{b\downarrow}^\dagger d_{a\downarrow} + d_{a\uparrow}^\dagger d_{b\downarrow} d_{a\downarrow}^\dagger d_{b\uparrow} \right). \quad (3)$$

Here, the index i for Ru sites is suppressed for simplicity. The matrix elements of \hat{U} and \hat{J} , evaluated by using the cRPA, are given by

$$\hat{U} = \begin{bmatrix} 5.236 & 4.260 & 4.196 \\ 4.260 & 5.236 & 4.196 \\ 4.196 & 4.196 & 5.482 \end{bmatrix} \quad (4)$$

and

$$\hat{J} = \begin{bmatrix} & 0.488 & 0.567 \\ 0.488 & & 0.567 \\ 0.567 & 0.567 & \end{bmatrix} \quad (5)$$

with the basis of $\{e'_{g1}, e'_{g2}, a_{1g}\}$.

-
- [1] J. C. Slater, Phys. Rev. **82**, 538 (1951).
- [2] N. F. Mott, Proc. Phys. Soc., London, Sect. A **62**, 416 (1949).
- [3] J. Hubbard, Proc. R. Soc., London, Sect. A **276**, 238 (1963).
- [4] P. W. Anderson, Phys. Rev. **79**, 350 (1950).
- [5] T. Takeda and S. Ōhara, J. Phys. Soc. Jpn. **37**, 275 (1974).
- [6] Y. G. Shi, Y. F. Guo, S. Yu, M. Arai, A. A. Belik, A. Sato, K. Yamaura, E. Takayama-Muromachi, H. F. Tian, H. X. Yang, J. Q. Li, T. Varga, J. F. Mitchell, and S. Okamoto, Phys. Rev. B **80**, 161104(R) (2009).
- [7] E. E. Rodriguez, F. Poineau, A. Llobet, B. J. Kennedy, M. Avdeev, G. J. Thorogood, M. L. Carter, R. Seshadri, D. J. Singh, and A. K. Cheetham, Phys. Rev. Lett. **106**, 067201 (2011).
- [8] J. Mravlje, M. Aichhorn, and A. Georges, Phys. Rev. Lett. **108**, 197202 (2012).
- [9] A. W. Sleight, J. L. Gilson, J. F. Weiher, and W. Bindloss, Solid State Commun. **14**, 357 (1974).
- [10] D. Mandrus, J. R. Thompson, R. Gaal, L. Forro, J. C. Bryan, B. C. Chakoumakos, L. M. Woods, B. C. Sales, R. S. Fishman, and V. Keppens, Phys. Rev. B **63**, 195104 (2001).
- [11] J. Yamaura, K. Ohgushi, H. Ohsumi, T. Hasegawa, I. Yamauchi, K. Sugimoto, S. Takeshita, A. Tokuda, M. Takata, M. Udagawa, M. Takigawa, H. Harima, T. Arima, and Z. Hiroi, Phys. Rev. Lett. **108**, 247205 (2012).
- [12] H. Shinaoka, T. Miyake, and S. Ishibashi, Phys. Rev. Lett. **108**, 247204 (2012).
- [13] I. M. Lifshitz, Sov. Phys. JETP **11**, 1130 (1960).
- [14] C. I. Hiley, M. R. Lees, J. M. Fisher, D. Thompsett, S. Agrestini, R. I. Smith, and R. I. Walton, Angew. Chem., Int. Ed. **53**, 4423 (2014).
- [15] W. Tian, C. Svoboda, M. Ochi, M. Matsuda, H. B. Cao, J.-G. Cheng, B. C. Sales, D. G. Mandrus, R. Arita, N. Trivedi, and J.-Q. Yan, Phys. Rev. B **92**, 100404(R) (2015).
- [16] C. I. Hiley, D. O. Scanlon, A. A. Sokol, S. M. Woodley, A. M. Ganose, S. Sangiao, J. M. De Teresa, P. Manuel, D. D. Khalyavin, M. Walker, M. R. Lees, and R. I. Walton, Phys. Rev. B **92**, 104413 (2015).
- [17] D. J. Singh, Phys. Rev. B **91**, 214420 (2015).
- [18] S. Streltsov, I. I. Mazin, and K. Foyevtsova, Phys. Rev. B **92**, 134408 (2015).
- [19] A. Georges, G. Kotliar, W. Krauth, and M. J. Rozenberg, Rev. Mod. Phys. **68**, 13 (1996).
- [20] V. I. Anisimov, A. I. Poteryaev, M. A. Korotin, A. O. Anokhin, and G. Kotliar, J. Phys. Condens. Matter **9**, 7359 (1997).
- [21] A. I. Lichtenstein and M. I. Katsnelson, Phys. Rev. B **57**, 6884 (1998).
- [22] G. Kotliar, S. Y. Savrasov, K. Haule, V. S. Oudovenko, O. Parcollet, and C. A. Marianetti, Rev. Mod. Phys. **78**, 865 (2006).
- [23] J. Spitaler *et al.*, The EXCITING FP-LAPW code: <http://exciting.sourceforge.net/>
- [24] N. Marzari and D. Vanderbilt, Phys. Rev. B **56**, 12847 (1997).
- [25] I. Souza, N. Marzari, and D. Vanderbilt, Phys. Rev. B **65**, 035109 (2001).
- [26] J. Kunes, R. Arita, P. Wissgott, A. Toschi, H. Ikeda, and K. Held, Comp. Phys. Commun. **181**, 1888 (2010).
- [27] A. A. Mostofi, J. R. Yates, Y.-S. Lee, I. Souza, D. Vanderbilt and N. Marzari, Comput. Phys. Commun. **178**, 685 (2008).
- [28] F. Aryasetiawan, M. Imada, A. Georges, G. Kotliar, S. Biermann, and A. I. Lichtenstein, Phys. Rev. B **70**, 195104 (2004).
- [29] P. Werner, A. Comanac, L. De Medici, M. Troyer, A. J. Millis, Phys. Rev. Lett. **97**, 076405 (2006).
- [30] P. Werner and A. J. Millis, Phys. Rev. B **74**, 155107 (2006).
- [31] K. Haule, Phys. Rev. B **75**, 155113 (2007).
- [32] M. T. Czyzyk and G. A. Sawatzky, Phys. Rev. B **49**, 14211 (1994).
- [33] V. I. Anisimov, F. Aryasetiawan, and A. I. Lichtenstein, J. Phys. Condens. Matter **9**, 767 (1997).
- [34] A. I. Lichtenstein, M. I. Katsnelson, and G. Kotliar, Phys. Rev. Lett. **87**, 067205 (2001).
- [35] B. Amadon, F. Lechermann, A. Georges, F. Jollet, T. O. Wehling, and A. I. Lichtenstein, Phys. Rev. B **77**, 205112 (2008).
- [36] K. Haule, C.-H. Yee, and K. Kim, Phys. Rev. B **81**, 195107 (2010).
- [37] J. Kuneš, V. Křápek, N. Parragh, G. Sangiovanni, A. Toschi, and A. V. Kozhevnikov, Phys. Rev. Lett. **109**, 117206 (2012).
- [38] K. Haule, T. Birol, and G. Kotliar, Phys. Rev. B **90**, 075136 (2014).
- [39] K. Haule, Phys. Rev. Lett. **115**, 196403 (2015).
- [40] S. Okamoto and A. J. Millis, Phys. Rev. B **70**, 195120 (2004).
- [41] P. Werner and A. J. Millis, Phys. Rev. Lett. **99**, 126405 (2007).
- [42] L. de' Medici, S. R. Hassan, M. Capone, and X. Dai, Phys. Rev. Lett. **102**, 126401 (2009).
- [43] L. de' Medici, J. Mravlje, and A. Georges, Phys. Rev. Lett. **107**, 256401 (2011).
- [44] A. Georges, L. de' Medici, and J. Mravlje, Annu. Rev. Condens. Matter Phys. **4**, 137 (2013).
- [45] M. Jarrell and J. E. Gubernatis, Physics Reports **269**, 133 (1996).
- [46] P. Hansmann, R. Arita, A. Toschi, S. Sakai, G. Sangiovanni, and K. Held, Phys. Rev. Lett. **104**, 197002 (2010).
- [47] A. Toschi, R. Arita, P. Hansmann, G. Sangiovanni, and K. Held, Phys. Rev. B **86**, 064411 (2012).
- [48] M. Liu, L. W. Harriger, H. Luo, M. Wang, R. A. Ewings, T. Guidi, H. Park, K. Haule, G. Kotliar, S. M. Hayden, and P. Dai, Nature Phys. **8**, 376 (2012).
- [49] J.-G. Cheng (private communication).
- [50] J. P. Perdew and Y. Wang, Phys. Rev. B **45**, 13244 (1992).
- [51] A. Kozhevnikov, A. Eguluz, and T. Schulthess, SC'10 Proceedings of the 2010 ACM/IEEE International Conference for High Performance Computing, Networking, Storage, and Analysis (IEEE Computer Society, Washington, DC, 2010), pp. 1-10 (2010).

Acknowledgments

The research by S.O. and J.Y. is supported by the U.S. Department of Energy, Office of Science, Basic Energy Sciences, Materials Sciences and Engineering Division. This work was supported by JSPS KAKENHI Grants No. 15K17724 (M.O.) and 15H05883 (R.A.). N.T. acknowledges funding from Grant No. nsf-dmr1309461. This research was initiated at the Kavli Institute for Theoretical Physics (KITP), the University of California, Santa Barbara, where three of the authors (S.O, R.A. and N.T.) attended the program “New Phases and Emergent Phenomena in Correlated Materials with Strong Spin-Orbit

Coupling.” S.O., R.A. and N.T. thank the KITP, which is supported in part by the National Science Foundation under Grant No. NSF PHY11-25915, for hospitality.

Author contributions

S.O. designed the project, performed the DMFT calculations, and wrote the manuscript. M. O. and R. A. performed the DFT calculations. J. Y. and N. T. provided additional inputs. All the authors discussed the results.